Modelling the geodynamo: progress and challenges

Binod Sreenivasan

Department of Mechanical Engineering, Indian Institute of Technology-Kanpur, Kanpur 208 016, India

It is widely accepted that the Earth's magnetic field is powered by a convection-driven dynamo operating in its liquid iron core. The twentieth century witnessed remarkable advances in the field of magnetohydrodynamics, which eventually led to three-dimensional computer simulations of the geodynamo. In this review we look at the significant developments that shaped our present understanding of magnetic field generation in the Earth's core. We also examine the successes and shortcomings of current geodynamo models.

Keywords: Earth's core, geodynamo, geomagnetism, magnetohydrodynamics.

Introduction

THE Earth has a large-scale dipolar magnetic field, a fact of historical importance because of the role of the magnetic compass in the exploration of our planet. The magnetic lines of force originate from the magnetic North and South Poles, which are presently about 11.5° away from the geographic North and South Poles. The Earth's magnetic field acts as a shield against high-energy particles from the Sun and outer space, thereby protecting our atmosphere and the life that it supports. No better reason can be given for understanding the Earth's magnetic field and its evolution over 4 billion years. The Earth's field has varied considerably over geological time, sometimes being weak, sometimes strong and intermittently reversing direction completely, so that North becomes South and South becomes North. This pattern of changes, and notably the polarity flips, have left a distinctive fingerprint on the surface of the Earth. Palaeomagnetists examine rocks and seabed sediments which formed in ancient times to follow the long-time behaviour of the geomagnetic field. For instance, magnetic minerals crystallize in cooling lava flows and orientate themselves towards the magnetic North Pole. This magnetic record is permanently locked in the rocks when they harden. Data from volcanic rocks and sediments show that the last flip in magnetic field polarity occurred about 780,000 years ago. Direct vector measurements of the geomagnetic field were pioneered by Carl Friedrich Gauss in the 1830s, and since the 1960s an excellent global distribution of the field has been provided by satellites. However, at lengthscales shorter than 2600 km the core magnetic field is obscured by the remnant crustal field, thus limiting our knowledge of the field in the planet's deep interior.

The concept of *magnetic field generation* goes back to Michael Faraday, who showed that an electrical conductor moving in a static magnetic field produces an electric current. This was the principle behind his disk dynamo, which consisted of a conducting disk spinning in a magnetic field. The next step was to examine whether this induced electric current could, in turn, produce a magnetic field that reinforces the original field. A disk dynamo can be designed such that the induced electric current flows through a loop in the same direction as the sense of spin[1]; this results in an induced magnetic field that points in the same direction as the pre-existing field. It was Larmor[2] who first suggested that an electrically conducting fluid in which suitable motions were produced could sustain magnetic fields in the Sun and Earth. Earlier studies in seismology[3,4] had already led to the inference that the Earth's outer core is liquid because of its inability to transmit transverse (shear) waves. Hence Larmor's idea of a self-excited *fluid dynamo* was an attractive proposition for the Earth. Why do we need a dynamo theory for the Earth? If there were no fluid motions in the core, any primordial magnetic field would have decayed away on a timescale of $\sim 10^4$ years[1]. Yet, the Earth has had a magnetic field for $\sim 10^9$ years, which can be explained by a process of field generation through induction in its core. Fluid motion in the outer core is thought to be driven either by natural convection or by buoyant plumes of light material released from the boundary of the inner core as pure iron crystallizes[5]. The presence of dissolved radioactive heat sources cannot be ruled out. The iron-rich core ensures that the motion of the fluid in a magnetic field is an inductive process that generates new magnetic field through stretching and twisting of flux tubes by the background velocity, the process being limited by magnetic diffusion. Alternative mechanisms for generation of the Earth's magnetic field, such as thermoelectric and electrochemical effects, have been proposed, but they cannot plausibly provide the energy required to maintain the observed field.

e-mail: bsreeni@iitk.ac.in

Although observation of the Earth's magnetic field has a long history of over 400 years[6], geodynamo theory made significant progress only in the last century due to advances in the subject of magnetohydrodynamics (MHD), which deals with the flow of electrically conducting fluids in magnetic fields. The development of numerical methods and solutions and the advent of fast computers aided this progress. The self-consistent dynamo problem requires solution of the MHD equations, which simultaneously determine the magnetic field, velocity and temperature (or composition) in a conducting fluid. Recent advances in computational ability have enabled us to perform three-dimensional simulations of the geodynamo, which provide realizations of geomagnetic field features such as the dipolar structure, secular variation (time-changes of the magnetic field), high-latitude magnetic flux concentrations and polarity reversals. The aim of this article is to discuss the progress made over the decades in modelling the geodynamo and the challenges that lie ahead. This review is by no means exhaustive; aspects of the geodynamo not covered here can be found in earlier reviews[7–11].

Early developments in geodynamo theory

It was natural for early investigators to consider rotating MHD systems in which both the velocity and magnetic fields were axisymmetric. As the Earth's external field is essentially a dipole, one might look at a steady, axisymmetric dynamo in which the magnetic field **B** is poloidal, $(B_r, 0, B_z)$ in cylindrical polar coordinates (r, θ, z). The electric current **j** is then toroidal, $(0, j_\theta, 0)$. The velocity field **u** is also poloidal. Cowling[12] considered such an idealized system and concluded that an axisymmetric magnetic field could not be supported by axisymmetric fluid motions. His argument was that an axisymmetric poloidal field always has a neutral ring where **B**, and hence **j** are zero. This *anti-dynamo* theorem showed that nonaxisymmetric configurations had to be considered to make progress in dynamo theory. (It was, however, shown later that axisymmetric flows could support non-axisymmetric fields.) It was Elsasser[13] who initiated the study of the interaction between non-axisymmetric (three-dimensional) velocity and magnetic fields. He also suggested decomposing the two fields into poloidal and toroidal components and then expanding them in spherical harmonics. This approach was developed further by Bullard and Gellman[14] and is being used in dynamo models today. For instance,

$$\mathbf{u} = \nabla \times (T\mathbf{r}) + \nabla \times \nabla \times (P\mathbf{r}); \tag{1}$$

$$T(r, \theta, \phi, t) = \sum_{l=0}^{L} \sum_{m=-l}^{l} T_l^m(r, t) Y_l^m(\theta, \phi), \tag{2}$$

where T and P are the toroidal and poloidal components of **u** and Y_l^m is a normalized spherical harmonic function.

Bullard and Gellman outlined a cyclic process by which a poloidal magnetic field can regenerate itself (see pages 259–260 of their paper)[14]. A toroidal field is swept out from an existing poloidal field through differential rotation (Figure 1 *a*); and an upwelling followed by a twist recreates a poloidal field from a toroidal field (Figure 1 *b*). These two events came to be known as the ω-effect and the α-effect respectively. The concept of the α-effect was developed further by Parker[15], who suggested that the deformation of the toroidal field can happen in cyclones and anticyclones similar in structure to those found in the atmosphere. Steenbeck *et al.*[16] provided a mathematical framework for the α-effect by noting that a small-scale, non-axisymmetric velocity $\mathbf{u}'$ interacts with a small-scale magnetic field $\mathbf{b}'$ to generate a large-scale electromotive force $\overline{E} = \overline{\mathbf{u}' \times \mathbf{b}'}$, which, in turn, is proportional to the mean magnetic field $\mathbf{B}_0$. (The constant of proportionality here is denoted by α.) The small-scale motion can be generated in the Earth's core either by free convection or by buoyant blobs of light elements released from a mushy zone near the inner core boundary[5].

The popularity of the α-effect inevitably led to the *kinematic dynamo* problem[17–20], which addresses the question of whether a given flow can generate a magnetic field or not. The magnetic field is governed by Maxwell's equations and Ohm's law for a moving conductor[21]. Combining these gives the magnetic induction equation, which determines the evolution of **B**:

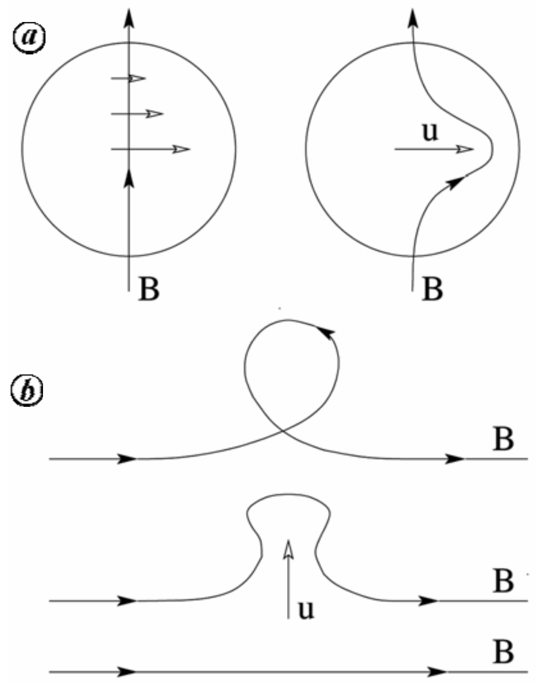

Figure 1. Schematic of the α–ω dynamo cycle[1,10,14]. ***a***, An initial poloidal field is swept by differential rotation to give a toroidal field; ***b***, Fluid motion lifts and twists a toroidal field line to produce a poloidal field loop.

$$\frac{\partial \mathbf{B}}{\partial t} = \nabla \times (\mathbf{u} \times \mathbf{B}) + \eta \nabla^2 \mathbf{B}, \tag{3}$$

where η is the magnetic diffusivity. Magnetic field growth happens when convection of **B**, given by the first term on the right-hand side, exceeds magnetic diffusion, given by the second term. The ratio of the two terms gives the magnetic Reynolds number, Rm = $u_* L/\eta$, where u_* is the typical velocity and L is the lengthscale.

Although kinematic dynamos have been successful in telling us which flows can produce magnetic fields resembling that of the Earth, they have ignored the effect of the magnetic field on the velocity. To ensure the coupled evolution of **u** and **B**, the induction equation (3) must be solved in conjunction with the momentum equation for a liquid metal. And if the flow is driven by, say, thermal convection, then the temperature must also be solved for.

We therefore have the additional equations,

$$\frac{\partial \mathbf{u}}{\partial t} + (\mathbf{u} \cdot \nabla)\mathbf{u} + 2\boldsymbol{\Omega} \times \mathbf{u} = -\frac{1}{\rho_0}\nabla p + \frac{\rho}{\rho_0}\mathbf{g} + \frac{1}{\rho_0 \mu_0}(\nabla \times \mathbf{B}) \times \mathbf{B} + \nu \nabla^2 \mathbf{u}, \tag{4}$$

$$\frac{\partial T}{\partial t} + (\mathbf{u} \cdot \nabla) T = \kappa \nabla^2 T + Q_s, \tag{5}$$

where **u** and **B** also satisfy the divergence-free conditions

$$\nabla \cdot \mathbf{u} = 0; \;\; \nabla \cdot \mathbf{B} = 0. \tag{6}$$

The terms on the left-hand side of eq. (4) represent linear and nonlinear inertia (which together give the material derivative $D\mathbf{u}/Dt$), and the Coriolis force. The forces on the right-hand side are, in order of appearance, the fluid pressure modified by centrifugal acceleration, buoyancy, magnetic (Lorentz) force and viscous diffusion. In the above equation, μ_0 is the permeability of free space, $(1/\mu_0)\nabla \times \mathbf{B}$ the current density **j** by Ampere's law, $\boldsymbol{\Omega}$ the background rotation vector that points in the z-direction, **g** the local gravity pointing downward, ρ and ρ_0 the local and far-field densities, κ the thermal diffusivity and Q_s a uniform volumetric heat source/sink.

Before discussing the solutions of the MHD eqs (3)–(6), a note on convection subject to rotation and magnetic field is appropriate.

Onset of convection and the effects of rotation and magnetic field

The classical problem of *Rayleigh–Bénard convection* consists of a fluid layer confined between two plates of infinite horizontal extent and heated from below. The difference in temperature across the layer, ΔT is related to the difference in density, $\Delta\rho$ via the *Boussinesq* approximation, which gives $\Delta\rho = -\rho_0 \beta \Delta T$, where β is the volumetric expansion coefficient and ρ_0 is the density at the upper boundary, where the temperature is T_0. As the temperature difference across the layer exceeds a critical value, up-and-down convective motions are set up. The driving force for these motions is buoyancy, which is the difference between the force of gravity acting on light and heavy fluid elements. Now, the effect of background rotation on this fluid layer may be understood by looking at the curl of the momentum conservation eq. (4) for an incompressible fluid incorporating the Boussinesq approximation:

$$\frac{\partial \boldsymbol{\omega}}{\partial t} + \mathbf{u} \cdot \nabla \boldsymbol{\omega} - (2\boldsymbol{\Omega} + \boldsymbol{\omega}) \cdot \nabla \mathbf{u} = \nabla \times g\beta T \hat{\mathbf{z}} + \frac{1}{\mu_0 \rho_0} \nabla \times [(\nabla \times \mathbf{B}) \times \mathbf{B}] + \nu \nabla^2 \boldsymbol{\omega}, \tag{7}$$

where $\boldsymbol{\omega}$ is the vorticity. T is the total temperature, which is the sum of the basic state (conductive) temperature and the deviation from this state. If we consider slow and steady motions in an inviscid fluid and assume there are no body forces arising either from the magnetic field or from temperature (or density) perturbations, then we immediately obtain $2\Omega \partial \mathbf{u}/\partial z = 0$, the famous *Proudman–Taylor theorem*[22,23]. This axial invariance of velocity is also known as the *geostrophic* state, where the Coriolis force $2\rho_0 \boldsymbol{\Omega} \times \mathbf{u}$ is in exact balance with the horizontal pressure gradient $-\nabla p$ in eq. (4). As the flow is purely two-dimensional, it cannot transmit heat across the fluid layer. Evidently, the onset of convection can occur only if the Proudman–Taylor (or rotational) constraint is broken, which would be the case if viscous diffusion is present[24]. The smaller the viscosity, the more difficult it is to start convection because the buoyancy forces must be large. In rotating convection the flow takes the form of rolls (Taylor columns) aligned with the axis of rotation. Later we shall look at the consequences of the Proudman–Taylor theorem for convection in the Earth's core.

We now consider the case when the above fluid layer is electrically conducting and permeated by a magnetic field, **B**. The Lorentz force in eq. (7) overcomes the rotational constraint by inducing velocity gradients via the Coriolis force $2\Omega \partial \mathbf{u}/\partial z$, a process that occurs even for zero viscosity. The effect of the magnetic field may also be understood from energy arguments. An axially varying azimuthal field causes axial variations in the lengthscale of the fluid columns perpendicular to $\boldsymbol{\Omega}$, with regions in a strong field being preferentially thicker than regions in a weak field. Any increase in lateral dimension of the columns would result in reduced energy dissipation, so that buoyancy does not have to work so hard to maintain convection[9]. The above role of the magnetic field in aiding rotating convection is in contrast to its role in non-rotating fluids where the field tends to suppress motions by Ohmic dissipation[25–27]. In summary, rotation tends to suppress convection, whereas the magnetic field makes it easier to set up convection in a rotating fluid.

Nonlinear convective geodynamo models

In a geodynamo model the fundamental MHD equations (3)–(6) are made dimensionless and then solved numerically for a Boussinesq fluid between two concentric spherical surfaces that mimic the Earth's inner core boundary (ICB) and the core-mantle boundary (CMB). The ratio of inner to outer radius, r_i/r_0 is usually chosen to be 0.35. The computational domain is shown schematically in Figure 2. The standard numerical method and boundary conditions have been discussed in previous papers[9,28]. We begin by looking at the dimensionless parameters.

Dimensionless parameters

The basic dimensionless groups used in dynamo models are the Ekman number, the Rayleigh number, the Prandtl number and the magnetic Prandtl number. (The magnetic Reynolds number, $Rm = uL/\eta$ is an intrinsic parameter.) The Ekman number, $E = \nu/2\Omega L^2$, is the ratio of the viscous to Coriolis forces and is $\sim 10^{-15}$ for the core. However, some authors replace the kinematic viscosity, ν by a *turbulent* eddy viscosity ν_T and propose $E \sim 10^{-9}$. The Rayleigh number for convection can have different definitions depending on the mode of heating; for differential heating (Figure 2) $Ra = g\beta\Delta TL^3/\nu\kappa$, where L is the gap-width of the spherical shell and κ the thermal diffusivity. In dynamo models the classical Rayleigh number is often multiplied by the Ekman number to give a 'modified' Rayleigh number[9], $Ra_M = g\beta\Delta TL/2\Omega\kappa$. Estimates for Ra in the core vary from approximately the critical value for onset of convection[29], Ra_c to several orders of magnitude above Ra_c (refs 30, 31) even if the turbulent value of the diffusivity κ_T is adopted in place of its molecular value. The Prandtl number, Pr is given by ν/κ and the magnetic Prandtl number, Pm is ν/η. The Roberts number, given by $q = PmPr^{-1} = \kappa/\eta$, is a popular dimensionless group in many models, with a molecular value of $\sim 10^{-6}$ and a turbulent value of order unity[31].

Present-day numerical geodynamo models mostly operate in the parameter regime $E \gtrsim 10^{-7}$, $Pr \sim 1$, $q = \kappa/\eta \gtrsim 0.05$ and $Ra/Ra_c \lesssim 100$.

Linear theory of rapidly rotating convection

The theory for the onset of convection under rapid rotation (in the low Ekman number limit) was originated nearly four decades ago[32,33] and developed further recently[34,35]. These analyses are linear in the sense that the nonlinear inertial term in the momentum equation is neglected. It has been shown that the critical wavenumber at onset of convection, m_c varies as $E^{-1/3}$ and the critical Rayleigh number, Ra_c varies as $E^{-4/3}$. (Here E is the Ekman number.) As E is lowered, the critical Rayleigh number increases and convection takes the form of several tall thin columns. In the limit $E \to 0$ (zero viscosity), Ra_c goes to infinity, implying that no convection can occur without viscosity[24]. The value of Ra_c obtained from the theory of convection is generally accepted as the reference state in numerical dynamo models: The value of Ra/Ra_c tells us how strongly a dynamo is driven. Although the magnetic field is known to reduce the value of Ra_c (see the section 'Onset of convection and the effects of rotation and magnetic field', above), it is not easy to evaluate the true value of Ra_c in a nonlinear dynamo.

Nonlinear dynamo models

Elsasser's idea of solving the three-dimensional dynamo problem had to wait until the mid-1990s, when the first numerical solutions for the MHD equations appeared. As early models had no hope of realizing Earth-like parameters, they used hyperdiffusion to absorb the energy in higher spherical harmonics (small scales)[36], but this

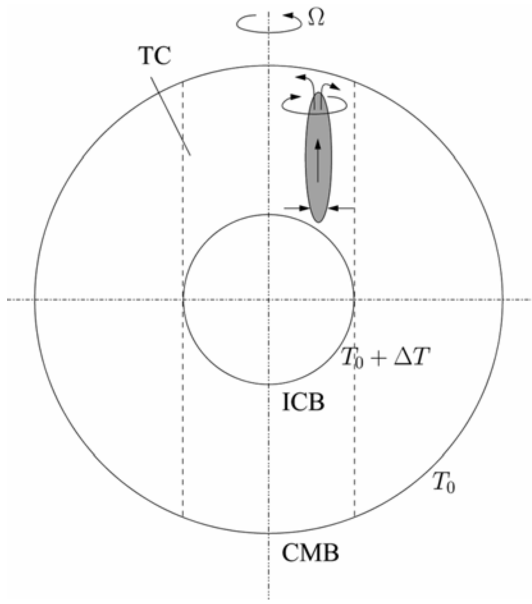

Figure 2. The dynamo equations are solved in a spherical shell whose boundaries represent the inner core boundary (ICB) of radius 1220 km and the core-mantle boundary (CMB) of radius 3480 km. The radii of the two boundaries for the Earth were determined from seismology[4,93]. The radius ratio of the fluid core 0.35 is used in geodynamo models. The dashed vertical lines represent the tangent cylinder (TC). In many models convection is driven by applying a temperature difference between the two boundaries. If convection inside TC takes the form of an off-axis plume, then an asymmetric, anticyclonic polar vortex is produced[50].

approach led to unphysical effects such as a much reduced azimuthal wavenumber[37]. Other models used a high Ekman number[38] or limited resolution in longitude[39], both of which helped reduce computational effort. These drawbacks were overcome in subsequent studies as computer speed increased. A simple convective dynamo, running from a prescribed initial state for temperature and magnetic field, has been adopted as the benchmark against which all dynamo codes can be tested for accuracy[40]. Dynamo models from the last decade have reproduced several Earth-like features like the dipolar magnetic field, secular variation and occasional field reversals.

Figure 3 shows snapshots of the flow and field produced in two dynamo simulations. The columnar structure of convection has origins in the Proudman–Taylor theorem for a rotating fluid; the number of columns increases with decreasing Ekman number, as predicted by linear theory[34]. At low E the magnetic field does not appear to thicken fluid columns, so the flow is essentially similar to that found in nonmagnetic convection. For $E = 5 \times 10^{-5}$ a westward drift is noted for both the velocity and magnetic fields, consistent with observations of secular variation[41,42]. The large-scale dipolar magnetic field appears to be generated in the fluid columns[43,44]. The strongly dipolar structure for $E = 1.5 \times 10^{-6}$ is not Earth-like (Figure 3 *b*), but a higher Rayleigh number might expel flux from the tangent cylinder. Models with

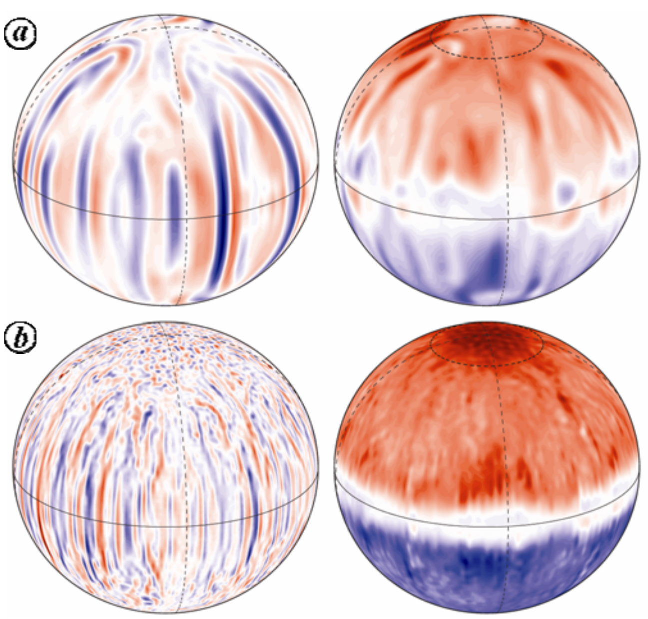

Figure 3. Contour plots for the radial velocity at $r = 0.8r_o$, where r_o is the outer radius (left panel), and the radial magnetic field at $r = r_o$ (right panel). All plots show longitudes spaced 90° apart and the equator. The thick dashed line in the field plots is the latitude at which the tangent cylinder cuts the core surface (≈ 70°). Positive values are shown in red and negative values in blue. ***a***, Dynamo model at $E = 5 \times 10^{-5}$, $Ra/Ra_c \approx 11$, $Pr = 1$ and $q = Pm = 1$. ***b***, Dynamo model at $E = 1.5 \times 10^{-6}$, $Ra/Ra_c \approx 50$, $Pr = 1$ and $q = Pm = 0.1$. See subsection 'Dimensionless parameters' for definitions of these parameters. No-slip, isothermal and electrically insulating boundary conditions are used in both models.

basal heating produce dipolar fields for a wide range of Ra/Ra_c, whereas those with uniform internal heating (used to mimic radioactive heat sources in the core) often produce non-dipolar fields as well[45].

Some dynamo models favour the α–ω dynamo cycle for field regeneration[46], whereas others favour an α^2 mechanism, where the toroidal field is produced by helical fluid motion in convection rolls[43,47] rather than by axial gradients in the azimuthal flow.

We shall now discuss how dynamo models have improved our understanding of core flows and magnetic fields.

Thermal winds and the mode of tangent cylinder convection

Temperature (density) perturbations in the Earth's core give rise to fluid motion whose behaviour can be predicted by considering the curl of the momentum eq. (7) in spherical polar coordinates (r, θ, ϕ), while retaining the conditions of slow and steady motion and negligible viscosity. For nonmagnetic convection,

$$2\Omega \frac{\partial u_\phi}{\partial z} = \frac{g\beta}{r} \frac{\partial T}{\partial \theta}; \tag{8}$$

$$2\Omega \frac{\partial u_\theta}{\partial z} = -\frac{g\beta}{\sin\theta} \frac{\partial T}{\partial \phi}. \tag{9}$$

The winds or currents implied by eqs (8) and (9) are known as the thermal wind, studied extensively in geophysical fluid dynamics[48]. In the northern hemisphere of the Earth's atmosphere, the temperature difference between the warm equatorial air and the cold Arctic air gives rise to a positive $\partial T/d\theta$, and the resulting jet stream that flows from west to east shortens flight times for aircraft travelling eastward. There is evidence from secular variation of the geomagnetic field that there are anticyclonic (westward) polar vortices in the core[49]. The origin of these vortices could be a thermal wind[50,51] caused by the polar regions in the core being warmer than the equatorial regions. Order-of-magnitude estimates show that even small latitudinal temperature variations (~ 10^{-3} K) can produce the observed anticyclonic vortices via eq. (8).

The magnitude of the thermal wind in the Earth is thought to be radically affected by its self-generated magnetic field. To understand this we must look at convection within the *tangent cylinder* (TC), an imaginary cylinder that touches the solid inner core of radius 1220 km, about 0.35 times the radius of the whole fluid core (see Figure 2). The rapid rotation of the Earth's core divides convection into two distinct regions, inside and outside the TC. Outside the TC convection occurs more readily than inside the TC because heat and composition can be convected outward by tall columns in which fluid motion is almost independent of the axial coordinate z, in an approximately geostrophic balance between the Coriolis force and the pressure gradient. (The CMB prevents complete geostrophy.) Inside the TC heat transport from the ICB to the CMB requires axial (z) motions that vary appreciably in the z-direction as both the ICB and CMB are impenetrable[44]. Numerical simulations of rotating convection and dynamos confirm that the Rayleigh number required for the onset of convection is much higher inside the TC than outside. When convection occurs in the TC, the flow often takes the form of a single coherent plume (hot spot) that extends from the inner boundary right up to the polar region, but offset from the rotation axis[50,44]; see Figure 2. The plume does not remain at the same longitude, but migrates in a rather irregular fashion, but generally westward. In nonmagnetic convection, however, the flow in the TC takes the form of tall thin columns whose radius is controlled by viscosity. In comparison with the *viscous mode* of convection, the *magnetic mode* produces stronger polar vortices which are non-axisymmetric (Figure 2). Interestingly, when nonlinear inertial forces are not small in the momentum equation (see below), the polar vortices become cyclonic, which suggests that inertial forces must be small enough in the Earth's core to make the vortices anticyclonic.

A couple of issues arise from the study of thermal winds. First, the variation of azimuthal velocity along z indicates not only that the flow may be anticyclonic at the poles, but also that it may be cyclonic near the ICB. This could result in a *superrotation* of the inner core relative to the mantle. There is some seismological evidence that the inner core is rotating faster than the mantle[52–54], but this is not conclusive[55]. On the other hand, gravitational coupling between the inner core and the mantle could prevent free relative motion between the two[56]. Another issue is that the magnetic field intensity in the poles is weak, whereas the field is concentrated in high-latitude flux lobes outside the TC (see below). While this could mean that convection inside the TC is too weak to generate a substantial field, it is more likely that strong magnetic-mode convection in the form of a plume expels flux from the polar regions.

How important is inertia for the Earth's core?

For large-scale motions in the Earth's core, we can estimate from eq. (4) that $|(\mathbf{u}\cdot\nabla)\mathbf{u}| \approx u_*^2/L$, where L is the typical lengthscale of the core, which we define as the difference between the outer and inner core radii $L = r_o - r_i \approx 2260$ km, and u_* a typical velocity of core motion. A velocity $u_* \sim 3\times10^{-4}$ is estimated from the observed secular variation based on the assumption that the field is frozen into the flow[1]. (Here we neglect magnetic diffusion in the induction eq. (3) and invert for the flow velocity at the core surface.) The *Rossby* number, which is the ratio of inertial to Coriolis forces in eq. (4) is then,

$$Ro = \frac{u_*}{L\Omega} \approx 2\times10^{-6} \ll 1. \tag{10}$$

Thus the flow in the core will be dominated by rotation even if the core velocities are somewhat larger than those observed near the CMB. It may be argued that the above argument underestimates the role of inertia if core convection takes the form of tall thin columns, as noted in Figure 3. If we suppose that the columns have extent $\sim L$ parallel to the rotation axis z, and a much shorter length $L_\perp$ perpendicular to the axis, then the curl of eq. (4) gives

$$|\nabla\times(\mathbf{u}\cdot\nabla)\mathbf{u}| \sim \frac{u_*^2}{L_\perp^2};\ |(\mathbf{\Omega}\cdot\nabla)\mathbf{u}| \sim \frac{\Omega u_*}{L}, \tag{11}$$

which gives a balance between the inertial and Coriolis terms when

$$L_\perp \approx L_R = \left(\frac{u_* L}{\Omega}\right)^{1/2} \sim 4\text{ km} \tag{12}$$

in the core. Here L_R is the *Rhines length*[57]. Motions on this scale are unlikely to be relevant to the dynamo process as magnetic fields on this lengthscale will decay in less than a year, assuming a value of $2\text{ m}^2\text{ s}^{-1}$ for the magnetic diffusivity[58]. Those columns that have had their horizontal scale enhanced by the effect of the magnetic field so that $L_\perp \gg L_R$ would be important for the geodynamo.

Numerical dynamo models can have inertia in them because it is not possible to solve the dynamo at realistic values of the Ekman number, E and magnetic Prandtl number, Pm. The Rossby number may be expressed as $Ro = EPm^{-1}Rm$. Dynamo models giving $Rm \sim 100$ frequently use $Pr = Pm = 1$ and $E \sim 10^{-4}$, so $Ro \sim 10^{-2}$. Recalling that the inertial force over a column can be enhanced significantly, the local value of the Rossby number can be much higher. Furthermore, if a low value of Pm is put into a dynamo code[45,59] Ro can easily be of order unity. It must be emphasized that these large values of Ro arise only because E has to be enhanced for numerical stability. A low value of E does allow a low value of Pm without increasing the magnitude of inertia[58,60]. (Also see the parameters for Figure 3*b*.) Sreenivasan and Jones[58] varied the Prandtl numbers Pr and Pm leaving other parameters fixed. For large $Pr = Pm$ they obtained a low-inertia solution for numerically accessible Ekman number. In this regime the dynamo is dipolar and the principal force balance is between the magnetic, Archimedean (buoyancy) and Coriolis forces, also known as the MAC balance. (For $E \sim 10^{-4}$ viscous forces are small except in the boundary layers where the velocity gradients are appreciable.) The MAC balance was envisaged for the geodynamo by Taylor[61] and Braginsky[62]. As

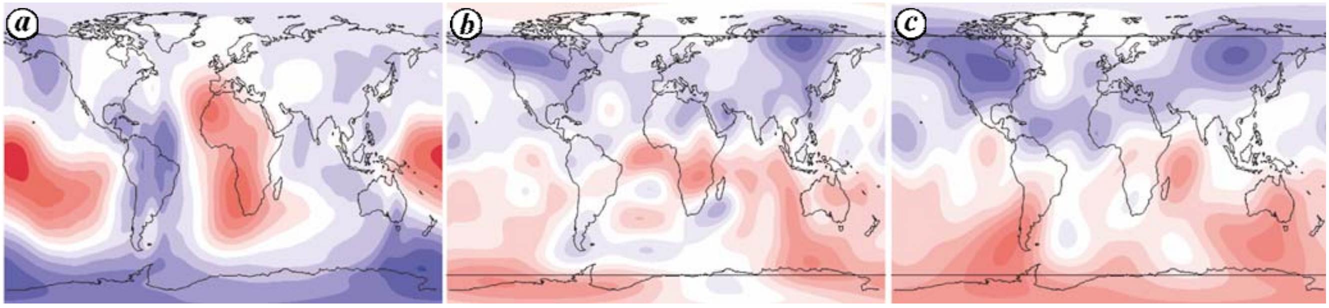

Figure 4. Spherical surface plots shown on a rectangular plane with longitude on the horizontal axis and latitude on the vertical axis. ***a***, Boundary condition derived from seismic tomography[94]. Seismic shear wave velocity at the base of the mantle is linearly related to temperature in the lower-mantle boundary layer. Cold (blue) patches occurring at the longitudes of the Atlantic and India induce downwellings, whereas the hot (red) patches under Africa and the Pacific suppress convection. ***b***, Observed field at the core surface in 1990. ***c***, Radial magnetic field at the upper boundary from a geodynamo model. The maximum variation of heat flux at the upper boundary is 0.6 times its mean value. The parameters are $E = 1.2 \times 10^{-4}$, $Ra/Ra_c = 1.5$, $Pr = 1$ and $q = 10$. No-slip boundary conditions are used for the velocity. The inner boundary is electrically conducting and isothermal, whereas the outer boundary is electrically insulating. Reproduced from Willis *et al.*[78].

$Pr = Pm$ is reduced, inertial forces begin to gain importance and the MAC balance is disturbed. The magnetic field becomes weak and less dipolar, suggesting that the presence of inertia is not conducive to dipolar field generation. Moreover, cyclonic polar vortices are obtained in inertial models, whereas it is known that the Earth's polar vortices are anticyclonic. Olson and Christensen[63] identified a transition in a local Rossby number (defined based on the characteristic lengthscale of the flow) that demarcates the dipolar and multipolar regimes, and argued that the Earth lies close to this transition. Although their argument can explain polarity reversals in Earth's history, it requires inertia to be as large as a tenth of the Coriolis forces in the core.

Nonlinear inertia does play a role in torsional oscillations in the core, which are geostrophic motions on cylinders parallel to the rotation axis. These motions exchange angular momentum between the inner core and mantle on decadal timescales, and are thought to produce millisecond variations in the length of day (LOD)[64,65]. As the Coriolis and pressure forces are in balance for these flows, the Lorentz force must come into balance with inertia. Recent studies have shown that a boundary-locked dynamo also enforces the Lorentz-inertia balance in the momentum equation[66] (see below).

Modelling core–mantle coupling

Today's geomagnetic field at the core–mantle boundary has four main lobes symmetrically placed north and south of the equator. They are centred outside the Earth's tangent cylinder near 55° North and South, and are near regions of high seismic velocity in the adjacent mantle (see Figure 4*b*). They have not moved much during the historical period of direct observation[67,68] and also show up in the time average of palaeomagnetic data from the last few million years[69–71]. Lateral variations in the mantle are essential for any long-term non-axisymmetric features in the magnetic field: If the mantle were perfectly spherically symmetric, the core flow would be free to evolve relative to it, eliminating the possibility of preferred longitudes. Hide[72] was the first to suggest that the lower-mantle variations cast their signature on the morphology of the geomagnetic field. Cold regions in the lower mantle could cause preferential cooling of the core, downwelling, and concentration of vertical magnetic flux at the core surface. This qualitative suggestion has now been explored in many convection and dynamo models, mostly by imposing a thermal boundary condition with the same structure as a 'tomographic' model of shear wave velocity variation in the lowermost mantle (Figure 4*a*). The dominant pattern is a fast (cold) ring around the Pacific rim with slow (hot) regions beneath the Pacific and Africa. The largest term in a spherical harmonic expansion of the tomography is Y_2^2, and many studies have simplified the boundary condition to this equatorially symmetric harmonic.

Early numerical simulations of core–mantle interaction were on nonmagnetic convection with infinite Prandtl number (Pr) and laterally varying temperature boundary conditions. At slightly supercritical Rayleigh number the drifting pattern of fluid rolls becomes stationary, or 'locked' to the boundary, provided the lateral variation in boundary heating is sufficiently strong. It was suggested that locking occurs when the wavelength of convection with homogeneous boundary conditions is similar to the wavelength of the boundary anomalies[73]. Fully self-consistent geodynamo simulations with inhomogeneous thermal boundary conditions have since been used to explore boundary effects on the frequency of field reversals[74], secular variation of the geomagnetic field[75], the time-averaged magnetic field[76] and core surface flows[77]. These studies generally support the idea that lower-mantle shear wave velocity correlates with some aspects of the time-averaged field, but there is little evidence of any simple boundary locking in any of the results, nor is there any direct similarity between snapshots of the solutions and the present-day geomagnetic field. A dynamo solution in which the magnetic field was locked to the boundary anomalies defined by seismic tomography was obtained recently[78,79]. The solution was not stationary, but the characteristic four main lobes persisted for many diffusion times at the same sites as the main lobes of the geomagnetic field (Figure 4 *c*). However, the parameters at which boundary locking was obtained were not Earth-like: The Rayleigh number for convection had to be set to a low, marginally supercritical value; consequently the magnetic diffusivity in the model had to be kept to a tenth of the thermal diffusivity ($q = \kappa/\eta \sim 10$) to make a dynamo possible. To understand why a weakly convective parameter regime is crucial for locking, one must return to the thermal wind balance,

$$2\Omega \frac{\partial \mathbf{u}}{\partial z} = \nabla \times [g\beta T\mathbf{r}], \tag{13}$$

whose horizontal components were given by eqs (8) and (9). With boundary anomalies, the right-hand side of eq. (13) is made up of two parts, the temperature gradients produced by free convection and the temperature gradients originating from non-axisymmetric lateral variations at the boundary. Locking is obtained when the boundary-driven variations dominate the force balance. (Also see Figure 5.) Equation (13) is significant in that it allows fluid motion of *any wavenumber* to be produced by a prescribed thermal variation at the boundary. Previous studies had suggested that locking occurs when the wavenumber of convection is similar to the wavenumber of the boundary anomalies[73]. Clearly, no such matching of wavenumbers is required for locking produced by eq. (13) because it does not rely on convection in the first place!

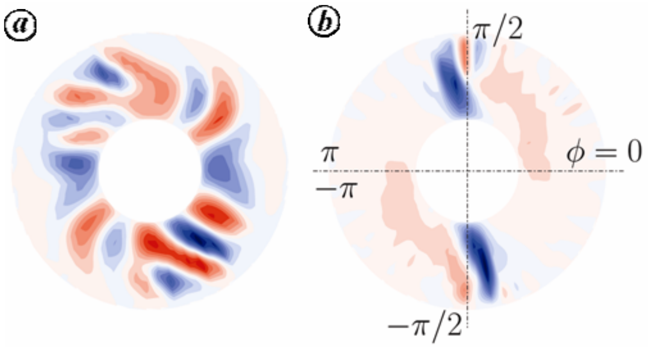

Figure 5. Radial velocity on the equatorial plane for (***a***) no lateral variation at the boundary and (***b***) a Y_2^2 variation in heat flux imposed at the upper boundary. The maximum variation of heat flux at the boundary is 1.6 times its mean value. The multicellular flow structure in (***a***) gives way to a locked, $m = 2$ structure in (***b***), where the wavenumber m is prescribed by the lateral variations at the boundary. The strong narrow downwellings are produced by the difference in absolute temperature at the upper boundary. The parameters are kept fixed at $E = 1 \times 10^{-4}$, $Ra/Ra_c = 1.5$, $Pr = 1$ and $q = 10$. Positive values are in red and negative values are in blue. No-slip boundary conditions are used for the velocity, the inner boundary is electrically conducting and isothermal and the outer boundary is electrically insulating. Reproduced from Sreenivasan[66].

How is locking affected by a high convective Rayleigh number and a low Ekman number? If the free convection-driven temperature gradients are stronger than the boundary-driven gradients in eq. (13), the velocity field is decoupled from the boundary and free to drift azimuthally. For low Ekman numbers locking looks progressively difficult. Since the critical Rayleigh number for onset of nonmagnetic convection increases with decreasing Ekman number ($Ra_c \sim E^{-4/3}$), even a marginally supercritical convective state can generate strong thermal winds that swamp the boundary variations. The above arguments led to a new model, where a combination of bottom heating and a uniform heat sink made convection much weaker at the top than at the bottom[80]. As boundary anomalies were allowed to dominate the thermal wind balance in the upper regions, partial locking of the flow and magnetic field was obtained. This model also obviated the need for a small magnetic diffusivity for dynamo action.

Recent studies on locked dynamos[66] have produced a few surprising results. First, the force balance is different from that in convection-driven dynamos. As the boundary-driven thermal wind balance is enforced, a secondary balance between the Lorentz and inertial forces follows, yielding an equipartition ($\mathbf{u} = \mathbf{B}$) solution[24]. That is, the kinetic and magnetic energies are equal, and the magnetic field and velocity field are tied together to one lengthscale. Although the Earth's magnetic field is not rigidly locked to lower-mantle variations, the above result does indicate that core–mantle coupling can place a constraint on the ratio of kinetic to magnetic energies. Secondly, lateral variations *by themselves* can, under small background convection, generate a magnetic field whose structure is fixed by the boundary wavenumber. This result suggests that lower-mantle variations might play a role in field generation.

Modelling geomagnetic field reversals

Geomagnetic reversals are perhaps the most interesting phenomena in geophysics, and perhaps the least understood. Magnetic records from ancient volcanic rock and sediments are our main source of information on reversals. The average reversal frequency in the last 20 Ma was about 5 every Ma, but the last reversal had occurred 0.78 Ma ago. From about 118–83 Ma ago, a period known as the *Cretaceous Superchron*, there are no recorded reversals of the field[81]. This period seems to show a significantly reduced secular variation[82], leading to speculation that the geodynamo was passing through a relatively stable phase. During reversals the axial dipole moment can decrease by a factor of 5 compared to its time-averaged value, and curiously, the dipole moment begins its decline 60–80 kyr before a reversal and recovers rapidly (within a few thousand years) after the dipole transition[83]. The geomagnetic dipole moment has been decreasing at a rapid rate in recent history[68,84], so the Earth might be in the early stage of a reversal[85].

The first polarity reversal in a geodynamo model was obtained by Glatzmaier and Roberts[86]. Since then several strongly driven dynamos have reported spontaneous polarity reversals[87–90], some reminiscent of palaeomagnetic reversals. Except for one model[89], most reversing dynamos have operated in a high Ekman number ($E \gtrsim 10^{-4}$) regime, which has been justified on grounds of simplicity and suitability for long simulations[91]. A high Ekman number is a natural choice for studying reversals as a strong convective state is realized for moderate Rayleigh numbers. A high-E, $Pm \sim 1$ dynamo has a Rossby number several orders of magnitude higher than that in the Earth, although it is claimed that the Rossby number based on the typical lengthscale of convection may not be far from the Earth's value. As the magnetic Reynolds number for flows of the Rhines lengthscale is only ~ 1, it is not clear that buoyancy will replenish vortices that are rapidly damped by the magnetic field.

Although the sequence of events during a dynamo reversal has been studied in several numerical models[88], the fundamental cause of field reversals is a mystery. An insight into departures from dipolar symmetry, including reversals, could perhaps be obtained by addressing the question of why rapidly rotating dynamos have a preference for dipolar solutions. We shall discuss this briefly in the concluding section.

The future of geodynamo modelling

Geodynamo models operating in vastly different parameter regimes have been successful in reproducing the main features of the geomagnetic field, the most important being the large-scale dipolar structure itself. This has provided the impetus to explore new dynamical regimes which are hopefully more Earth-like than previous models. The computationally difficult parameter space of low Ekman number and low Roberts number is explored on the supposition that it would be a better representation of core convection, but dynamos in this regime have not produced magnetic fields that look like the Earth. A fundamental study of the rapidly rotating regime should however be welcomed. Rotation with concomitant helical fluid motions in columns has been thought to produce dipolar fields, but recent studies suggest that magnetic field-induced flows can explain the preference for dipolar fields over quadrupolar fields (Sreenivasan and Jones, work in progress). These studies reaffirm our faith in nonlinear dynamos where the back-reaction of the magnetic field on the flow through the Lorentz force is given the importance it deserves. As we see below, they might also offer an insight into magnetic field reversals.

As convection in the Earth's core might take the form of tall columns parallel to the rotation axis, it makes sense to consider the axial component of the MAC force balance (see sub-section 'How important is inertia for the Earth's core?')

$$2\Omega \partial u_z/\partial z + g\beta \nabla \times (T\mathbf{r}) \cdot \hat{\mathbf{z}} + \nabla \times [(\nabla \times \mathbf{B}) \times \mathbf{B}] \cdot \hat{\mathbf{z}} = 0. \tag{14}$$

The point to note, however, is that the axial distribution of these forces is not uniform. The buoyancy force is strongest near the equator, where gravity acts perpendicular to the rolls and the temperature gradient is greatest. The peak of the damping Lorentz force, on the other hand, depends crucially on the peak of the azimuthal magnetic field B_ϕ, which for a dipolar field is not at the equator (where it is zero; see Figure 6 *a*), but at a point between the equator and the upper boundary. As the driving force and the damping force peak at different locations, it is inevitable that an axial velocity gradient is generated to satisfy a local force balance via eq. (14). This effect is manifest in Figure 6 *b*, where the Lorentz force enhances the axial kinetic energy in localized streaks. The growth in axial velocity contributes to an increase in *helicity* (the dot product of velocity and vorticity), an important quantity for dynamo action[1]. The field-induced flow is much weaker for a dynamo with a quadrupolar field because both damping and driving forces peak at the equator. We therefore have a mechanism giving strong preference for dipolar fields over quadrupolar fields. For a field reversal to occur, it is perhaps necessary to be in a strongly convecting regime, where

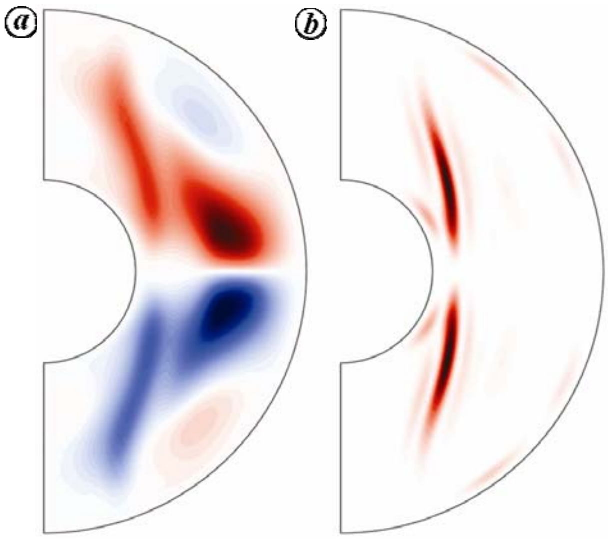

Figure 6. Azimuthally averaged meridional plots for a dynamo model at $E = 5 \times 10^{-5}$, $Ra/Ra_c \approx 6$, $Pr = 1$ and $q = Pm = 1$. Positive values are shown in red and negative values in blue. ***a***, Azimuthal magnetic field, B_ϕ. ***b***, Axial kinetic energy density, $\frac{1}{2}u_z^2$. No-slip, isothermal and electrically insulating boundary conditions are used. This model produces a stable, dipolar magnetic field.

the buoyancy force in regions away from the equator is large enough to cancel the effect of the Lorentz force, so that the production of $\partial u_z/\partial z$ in eq. (14) is inhibited. This mechanism of breakdown of dipolar symmetry must be tested in future dynamo models.

Dynamo models are a powerful tool for testing various other hypotheses for the Earth's core. For example, the possibility of driving a dynamo at least in part by lateral variations in the lower mantle suggests that the Rayleigh number for convection need not be high. A related issue is whether convection occurs everywhere in the core. We know from simulations that polarity reversals are realizable only in strongly driven dynamos. On the other hand, persistent core–mantle coupling through the boundary-driven thermal wind can only be obtained when convection is small. These two extreme regimes could coexist in a stably stratified model where convection is strong at depth but boundary anomalies control fluid motion in the upper regions[66,80], a scenario consistent with independent arguments based on compositional buoyancy[92]. It is a matter of concern that many models might be using unphysical basic state buoyancy profiles, prescribing either uniform heat flux throughout the core, or even worse, heat flux that increases from the ICB to the CMB.

Geodynamo models will be called upon in future to alleviate the deficiencies in our understanding of secular variation, field reversals, torsional oscillations and lower-mantle effects. Our understanding of the Earth's dynamo is far from complete, but with improved geophysical data from satellite missions and insights from laboratory experiments we can hope that newer models will emerge to provide useful comparisons with the observed geomagnetic field.

1. Moffatt, H. K., *Magnetic Field Generation in Electrically Conducting Fluids*, Cambridge University Press, 1978.
2. Larmor, J., How could a rotating body such as the Sun become a magnet? *Brit. Assn. Adv. Sci. Rep*., 1919, 159–160.
3. Oldham, R. D., The constitution of the Earth as revealed by earthquakes. *Quarternary J. Geol. Soc.*, 1906, **62**, 456–475.
4. Gutenberg, B., Uber die Konstitution der Erdinnern, erschlossen aus Erdbebenbeobachtungen. *Phys. Z.*, 1913, **14**, 1217–1218.
5. Moffatt, H. K. and Loper, D. E., The magnetostrophic rise of a buoyant parcel in the Earth's core. *Geophys. J. Int.*, 1994, **117**, 394–402.
6. Jonkers, A. R. T., Jackson, A. and Murray, A., Four centuries of geomagnetic data from historical records. *Rev. Geophys.*, 2003, **41**, 1006.
7. Busse, F. H., Homogeneous dynamos in planetary cores and in the laboratory. *Annu. Rev. Fluid Mech.*, 2000, **32**, 383–408.
8. Dormy, E., Valet, J. P. and Courtillot, V., Numerical models of the geodynamo and observational constraints. *Geochem. Geophys. Geosyst*., 2000, **1**, 1037.
9. Kono, M. and Roberts, P. H., Recent geodynamo simulations and observations of the geomagnetic field. *Rev. Geophys.*, 2002, **40**, 1013.
10. Roberts, P. H., Theory of the geodynamo. In *Treatise on Geophysics* (ed. Olson, P.), Elsevier, Amsterdam, 2007, vol. 8, pp. 67–102.
11. Jones, C. A., Thermal and compositional convection in the outer core. In *Treatise on Geophysics* (ed. Olson, P.), Elsevier, Amsterdam, 2007, vol. 8, pp. 131–185.
12. Cowling, T. G., The magnetic field of sunspots. *Mon. Not. Roy. Astron. Soc.*, 1934, **94**, 39–48.
13. Elsasser, W. M., Induction effects in terrestrial magnetism, Part I. Theory. *Phys. Rev*., 1946, **69**, 106–116.
14. Bullard, E. and Gellman, H., Homogeneous dynamos and terrestrial magnetism. *Philos. Trans. R. Soc. A*, 1954, **247**, 213–278.
15. Parker, E. N., Hydromagnetic dynamo models. *Astrophys. J.*, 1955, **122**, 293–314.
16. Steenbeck, M., Krause, F. and Rädler, K. H., A calculation of the mean electromotive force in an electrically conducting fluid in turbulent motion, under the influence of Coriolis forces. *Z. Naturforsch.*, 1966, **A21**, 369–376.
17. Gubbins, D., Numerical solutions of the kinematic dynamo problem. *Philos. Trans. R. Soc. London A*, 1973, **274**, 493–521.
18. Kumar, S. and Roberts, P. H., A three-dimensional kinematic dynamo. *Proc. R. Soc. London A*, 1975, **344**, 235–258.
19. Dudley, M. L. and James, R. W., Time-dependent kinematic dynamos with stationary flows. *Proc. R. Soc. London A*, 1989, **425**, 407–429.
20. Sarson, G. R. and Gubbins, D., Three-dimensional kinematic dynamos dominated by strong differential rotation. *J. Fluid Mech.*, 1996, **306**, 223–265.
21. Davidson, P. A., *An Introduction to Magnetohydrodynamics*, Cambridge University Press, 2001.
22. Proudman, J., On the motion of solids in a liquid possessing vorticity. *Proc. R. Soc. London A*, 1916, **92**, 408–424.
23. Taylor, G. I., The motion of a sphere in a rotating liquid. *Proc. R. Soc. London A*, 1923, **102**, 180–189.
24. Chandrasekhar, S., *Hydrodynamic and Hydromagnetic Stability*, Clarendon Press, Oxford, 1961.
25. Moreau, R., *Magnetohydrodynamics*, Kluwer Academic, Dordrecht, 1990.
26. Sreenivasan, B. and Alboussière, T., Experimental study of a vortex in a magnetic field. *J. Fluid Mech.*, 2002, **464**, 287–309.
27. Sreenivasan, B., Davidson, P. A. and Etay, J., On the control of surface waves by a vertical magnetic field. *Phys. Fluids*, 2005, **17**, 117101.
28. Clune, T. C., Elliot, J. R., Miesch, M. S., Toomre, J. and Glatzmaier, G. A., Computational aspects of a code to study rotating turbulent convection in spherical shells. *Parallel Computing*, 1999, **25**, 361–380.
29. Gubbins, D., The Rayleigh number for convection in the Earth's core. *Phys. Earth Planet. Int.*, 2001, **128**, 3–12.
30. Olson, P., Thermal interaction of the core and mantle. In *Earth's Core and Lower Mantle*, vol. 11 of *The Fluid Mechanics of Astrophysics and Geophysics* (eds Jones, C. A., Soward, A. M. and Zhang, K.), Taylor & Francis, London, 2003, pp. 1–38.
31. Anufriev, A. P., Jones, C. A. and Soward, A. M., The Boussinesq and anelastic liquid approximations for convection in the Earth's core. *Phys. Earth Planet. Int.*, 2005, **152**, 163–190.
32. Roberts, P. H., On the thermal instability of a rotating fluid sphere containing heat sources. *Philos. Trans. R. Soc. London A*, 1968, **266**, 535–558.
33. Busse, F. H., Thermal instabilities in rapidly rotating systems. *J. Fluid Mech*., 1970, **44**, 441–460.
34. Jones, C. A., Soward, A. M. and Mussa, A. I., The onset of thermal convection in a rapidly rotating sphere. *J. Fluid Mech.*, 2000, **405**, 157–179.
35. Dormy, E., Soward, A. M., Jones, C. A. and Cardin, P., The onset of thermal convection in rapidly rotating shells. *J. Fluid Mech*., 2004, **501**, 43–70.
36. Glatzmaier, G. A. and Roberts, P. H., A three-dimensional convective dynamo solution with rotating and finitely conducting inner core and mantle. *Phys. Earth Planet. Int*., 1995, **91**, 63–75.

37. Zhang, K. and Jones, C. A., The effect of hyperviscosity on geodynamo models. *Geophys. Res. Lett*., 1997, **24**, 2869–2872.
38. Kageyama, A., Sato, T. and the Complexity Simulation Group, Computer simulation of a magnetohydrodynamic dynamo. *Phys. Plasmas*, 1995, **2**, 1421–1431.
39. Jones, C. A., Longbottom, A. W. and Hollerbach, R., A self-consistent convection driven dynamo model, using a mean field approximation. *Phys. Earth Planet. Int.*, 1995, **92**, 119–141.
40. Christensen, U. *et al.*, A numerical dynamo benchmark. *Phys. Earth Planet. Int.*, 2001, **128**, 25–34.
41. Yukutake, T., The westward drift of the Earth’s magnetic field in historic times. *J. Geomagn. Geoelectr*., 1967, **19**, 103–116.
42. Dumberry, M. and Finlay, C. C., Eastward and westward drift of the Earth’s magnetic field for the last three millennia. *Earth Planet. Sci. Lett.*, 2007, **254**, 146–157.
43. Olson, P., Christensen, U. and Glatzmaier, G. A., Numerical modelling of the geodynamo: mechanisms of field generation and equilibration. *J. Geophys. Res*., 1999, **104**, 10383–10404.
44. Sreenivasan, B. and Jones, C. A., Azimuthal winds, convection and dynamo action in the polar regions of planetary cores. *Geophys. Astrophys. Fluid Dynam*., 2006, **100**, 319–339.
45. Grote, E., Busse, F. H. and Tilgner, A., Regular and chaotic spherical dynamos. *Phys. Earth Planet. Inter*., 2000, **117**, 259–272.
46. Kageyama, A. and Sato, T., Velocity and magnetic field structures in a magnetohydrodynamic dynamo. *Phys. Rev. E*, 1997, **55**, 4617–4626.
47. Christensen, U., Olson, P. and Glatzmaier, G. A., Numerical modelling of the geodynamo: a systematic parameter study. *Geophys. J. Int.*, 1999, **138**, 393–409.
48. Pedlosky, J., *Geophysical Fluid Dynamics*, Springer-Verlag, New York, 1987.
49. Olson, P. and Aurnou, J., A polar vortex in the Earth’s core. *Nature*, 1999, **402**, 170–173.
50. Sreenivasan, B. and Jones, C. A., Structure and dynamics of the polar vortex in the Earth’s core. *Geophys. Res. Lett*., 2005, **32**, L20301.
51. Aurnou, J., Andreadis, S., Zhou, L. and Olson, P., Experiments on convection in the Earth’s core tamgent cylinder. *Earth Planet. Sci. Lett*., 2003, **212**, 119–134.
52. Song, X. D. and Richards, P. G., Seismological evidence for differential rotation of the Earth’s inner core. *Nature*, 1996, **382**, 221–224.
53. Su, W., Dziewonski, A. M. and Jeanloz, R., Planet within a planet: rotation of the inner core of Earth. *Science*, 1996, **274**, 1883–1887.
54. Zhang, J., Song, X., Li, Y., Richards, P. G., Sun, X. and Waldhauser, F., Inner core differential motion confirmed by earthquake waveform doublets. *Science*, 2005, **309**, 1357–1360.
55. Souriau, A., Roudil, P. and Moynot, B., Inner core differential rotation: Facts and artefacts. *Geophys. Res. Lett.*, 1997, **24**, 2103–2106.
56. Buffett, B. A. and Glatzmaier, G. A., Gravitational braking of inner core rotation in geodynamo simulations. *Geophys. Res. Lett*., 2000, **27**, 3125–3128.
57. Rhines, P. B., Waves and turbulence on a beta-plane. *J. Fluid Mech*., 1975, **69**, 417–443.
58. Sreenivasan, B. and Jones, C. A., The role of inertia in the evolution of spherical dynamos. *Geophys. J. Int.*, 2006, **164**, 467–476.
59. Simitev, R. and Busse, F. H., Prandtl number dependence of convection-driven dynamos in rotating spherical fluid shells. *J. Fluid Mech*., 2005, **532**, 365–388.
60. Christensen, U. R. and Aubert, J., Scaling properties of convection-driven dynamos in rotating spherical shells and application to planetary magnetic fields. *Geophys. J. Int*., 2006, **166**, 97–114.
61. Taylor, J. B., The magneto-hydrodynamics of a rotating fluid and the Earth’s dynamo problem. *Proc. R. Soc*., 1963, **274**, 274–283.
62. Braginsky, S. I., Magnetic waves in the Earth’s core. *Geomagn. Aeoron*., 1967, **7**, 851–859.
63. Olson, P. and Christensen, U. R., Dipole moment scaling for convection-driven planetary dynamos. *Earth Planet. Sci. Lett.*, 2006, **250**, 561–571.
64. Jault, D., Gire, C. and Le Mouël, J. L., Westward drift, core motions and exchanges of angular momentum between core and mantle. *Nature*, 1988, **333**, 353–356.
65. Jault, D., Electromagnetic and topographic coupling, and LOD variations. In *Earth’s Core and Lower Mantle*, vol. 11 of *The Fluid Mechanics of Astrophysics and Geophysics* (eds Jones, C. A., Soward, A. M. and Zhang, K.), Taylor & Francis, London, 2003, pp. 56–76.
66. Sreenivasan, B., On dynamo action produced by boundary thermal coupling. *Phys. Earth Planet. Int*., 2009, **177**, 130–138.
67. Bloxham, J. and Gubbins, D., Thermal core-mantle interactions. *Nature*, 1987, **325**, 511–513.
68. Jackson, A., Jonkers, A. R. T. and Walker, M. R., Four centuries of geomagnetic secular variation from historical records. *Philos. Trans. R. Soc. London, Ser. A*, 2000, **358**, 957–990.
69. Johnson, C. and Constable, C., The time-averaged geomagnetic field as recorded by lava flows over the past 5 Myr. *Geophys. J. Int*., 1995, **122**, 489–519.
70. Carlut, J. and Courtillot, V., How complex is the time-averaged geomagnetic field over the past 5 Myr? *Geophys. J. Int*., 1998, **134**, 527–544.
71. Johnson, C. L., Constable, C. G. and Tauxe, L., Mapping long-term changes in Earth’s magnetic field. *Science*, 2003, **300**, 2044–2045.
72. Hide, R., Motions of the Earth’s core and mantle, and variations of the main geomagnetic field. *Science*, 1967, **157**, 55–56.
73. Zhang, K. and Gubbins, D., Convection in a rotating spherical fluid shell with an inhomogeneous temperature boundary condition at infinite Prandtl number. *J. Fluid Mech*., 1993, **250**, 209–232.
74. Glatzmaier, G. A., Coe, R. S., Hongre, L. and Roberts, P. H., The role of the Earth’s mantle in controlling the frequency of geomagnetic reversals. *Nature*, 1999, **401**, 885–890.
75. Christensen, U. R. and Olson, P., Secular variation in numerical geodynamo models with lateral variations of boundary heat flow. *Phys. Earth Planet. Int*., 2003, **138**, 39–54.
76. Olson, P. and Christensen, U., The time-averaged magnetic field in numerical dynamos with non-uniform boundary heat flow. *Geophys. J. Int.*, 2002, **151**, 809–823.
77. Aubert, J., Amit, H. and Hulot, G., Detecting thermal boundary control in surface flows from numerical dynamos. *Phys. Earth Planet. Inter.*, 2007, **160**, 143–156.
78. Willis, A. P., Sreenivasan, B. and Gubbins, D., Thermal core-mantle interaction: exploring regimes for ‘locked’ dynamo action. *Phys. Earth Planet. Inter*., 2007, **165**, 83–92.
79. Gubbins, D., Willis, A. P. and Sreenivasan, B., Correlation of Earth’s magnetic field with lower mantle thermal and seismic structure. *Phys. Earth Planet. Inter*., 2007, **162**, 256–260.
80. Sreenivasan, B. and Gubbins, D., Dynamos with weakly convecting outer layers: implications for core–mantle boundary interaction. *Geophys. Astrophys. Fluid Dynam*., 2008, **102**, 395–407.
81. Merrill, R. T. and McFadden, P. L., Geomagnetic field stability: Reversal events and excursions. *Earth Planet. Sci. Lett*., 1994, **121**, 57–69.
82. McFadden, P. L. and Merrill, R. T., Fundamental transitions of the geodynamo as suggested by palaeomagnetic data. *Phys. Earth Planet. Int*., 1995, **91**, 253–260.
83. Valet, J. P., Meynadier, L. and Guyodo, Y., Geomagnetic dipole strength and reversal rate over the past two million years. *Nature*, 2005, **435**, 802–805.
84. Olson, P. and Amit, H., Changes in Earth’s dipole. *Naturwissenschaften*, 2006, **93**, 11519–11542.

85. Constable, C. G. and Korte, M., Is Earth's magnetic field reversing? *Earth Planet. Sci. Lett*., 2006, **246**, 1–16.
86. Glatzmaier, G. A. and Roberts, P. H., A three-dimensional self-consistent computer simulation of a geomagnetic field reversal. *Nature*, 1995, **377**, 203–209.
87. Kutzner, C. and Christensen, U. R., From stable dipolar towards reversing numerical dynamos. *Phys. Earth Planet. Int*., 2002, **131**, 29–45.
88. Wicht, J. and Olson, P., A detailed study of the polarity reversal mechanism in a numerical dynamo model. *Geochem. Geophys. Geosyst*., 2004, **5**, Q03H10.
89. Takahashi, F., Matsushima, M. and Honkura, Y., A numerical study on magnetic polarity transition in an MHD dynamo model. *Earth Planets Space*, 2007, **59**, 665–672.
90. Rotvig, J., An investigation of reversing numerical dynamos driven by either differential or volumetric heating. *Phys. Earth Planet. Int*., 2009, **176**, 69–82.
91. Olson, P., Driscoll, P. and Amit, H., Dipole collapse and reversal precursors in a numerical dynamo. *Phys. Earth Planet. Int*., 2009, **173**, 121–140.
92. Fearn, D. R. and Loper, D. E., Compositional convection and stratification of Earth's core. *Nature*, 1981, **289**, 393–394.
93. Lehmann, I. P., *Bureau Central Séismologique International Strasbourg: Publications du Bureau Central Scientifiques*, 1936, **14**, 87–115.
94. Masters, T. G., Johnson, S., Laske, G. and Bolton, H. F., A shear-velocity model of the mantle. *Philos. Trans. R. Soc. London A*, 1996, **354**, 1385–1411.